ON GRID GENERATION FOR NUMERICAL MODELS
OF ATMOSPHERIC MODELING AND FORECASTING

Ludmila Bourchtein, Andrei Bourchtein*
Institute of Physics and Mathematics, Pelotas State University, Brazil

1. INTRODUCTION

Large-scale geophysical processes including synoptic variability, global atmospheric and oceanic circulation, and climate dynamics imply formulation of related mathematical models in spherical geometry. The approximate solutions to these complex models are usually found by applying numerical methods and their quality depends on principal properties of numerical schemes: accuracy, stability and efficiency.

Generation of the computational grids is an important step for definition of the scheme properties. For regional models or chosen regions of global domain, the best possible uniformity of computational grid is frequently required because it assures the highest accuracy and stability for dynamical part and the most justified choice of the parameterization schemes for physical part of numerical model. Computational grids based on spherical coordinates are highly nonuniform, which causes the problems for both dynamical and physical parts of numerical schemes. In fact, an accuracy of any scheme depends on the greatest physical mesh sizes in the chosen domain and, therefore, nonuniform physical grids lead to the loss of accuracy in the greatest mesh size subdomains or unnecessary refinement in the smallest mesh size subdomains. Furthermore, absolute majority of the schemes used in atmosphere and ocean dynamics are explicit or semi-implicit and, therefore, their time steps must be proportional to space mesh size to satisfy the numerical stability criterion. Hence, excessive refinement of spatial resolution can impose physically unjustified restriction on the allowable time step. Other problems of nonuniform resolution are related to physical parameterizations used in a model. The choice of the parameterization scheme could be problematic because of different definition of subgrid scales in the regions with different physical mesh sizes. Thus, the most uniform computational grid over the considered domain assures more efficient numerical scheme with more reliable solutions.

* _Corresponding author address_: Andrei Bourchtein, Pelotas State University, Institute of Physics and Mathematics, Campus Universitario da UFPel, Capao do Leao 96010-900, Brazil; e-mail: burstein@terra.com.br

Different approaches used to solve this problem can be classified according to type of transformation of a sphere in the following way: conformal mappings from sphere onto plane, non-conformal mappings onto plane (such as gnomonic, icosahedral and geodesic grids) and conformal mappings from a sphere onto a sphere (Williamson 1979, Staniforth 1997, Pearson 1990, Bygaevskiy and Snyder 1995). Conformal mapping onto a plane is most widespread approach because it allows us to keep a simpler form of the primitive equations and guarantees locally isotropic treatment of derivatives and smoothness of physical mesh size variation. Commonly used conformal projections are stereographic, conic and cylindrical. The stereographic projections are frequently applied to high and middle latitude regions (Benoit et al. 1997, Grell et al. 1994, Robert et al. 1985, Staniforth 1997, Tanguay 1989). They allow us to introduce more uniform grids than in the spherical coordinates as well as to eliminate the pole problem. The conic and cylindrical projections (Lambert and Mercator projections) are used for medium latitudes and tropical regions (Bourchtein 2002, Leslie and Purser 1991, MacDonald et al. 2000, Staniforth 1997). All these conformal mappings can be tangent or secant depending on the type of intersection of sphere with plane, cone or cylinder.

If conformal mappings are based on geographical (polar) latitude-longitude coordinates then they are called polar projections, otherwise, they are called rotated or oblique projections (Pearson 1990, Bugayevskiy and Snyder 1995, Staniforth 1997). The rotated spherical coordinates and conformal projections can be obtained from the polar ones by moving the pole to the chosen point. For example, the rotated spherical coordinates are used in the regional models by Mesinger et al. (1988) and McDonald and Haugen (1992) where the central point of considered region is chosen as the intersection of "equator" and the "first" meridian of the new rotated spherical coordinates. The rotated spherical coordinates are also used in the polar regions of the global models (Bates et al. 1993, McDonald and Bates 1989).

This paper is structured as follows. In section 2 we introduce an important characteristic for quantitative measure of the grid uniformity. In section 3 some analytical solutions

to problem of uniform grid generation are presented for simple spherical domains in the form of spherical disks. The Chebyshev-Milnor theory is applied to computation of the mappings with the minimum possible distortion over more complex domains, including the South America territory, in section 4. Finally, comparison between uniformity of conformal and orthogonal grids for spherical disks is presented in section 5.

2. PROBLEM FORMULATION AND PRINCIPAL CONCEPTS

The problems of grid generation for hydrostatic and non-hydrostatic atmospheric models considered over spherical regions can be illustrated by study of the shallow water equations. In fact, all coordinate transformations to be studied deal with surface mappings and, therefore, all vertical operators are invariant under these transformations.

The primitive shallow water equations in the geographical longitude-colatitude spherical coordinates λ and θ have the following form (Williamson 1979):

$$\frac{du}{dt} - \left(f + \frac{u}{a}\cot\theta\right)v = -\frac{1}{a\sin\theta}\frac{\partial\Phi}{\partial\lambda} \ ,$$

$$\frac{dv}{dt} + \left(f + \frac{u}{a}\cot\theta\right)u = -\frac{1}{a}\frac{\partial\Phi}{\partial\theta} \ ,$$

$$\frac{d\Phi}{dt} = -\Phi\frac{1}{a\sin\theta}\left(\frac{\partial u}{\partial\lambda} + \frac{\partial(v\sin\theta)}{\partial\theta}\right) \ . \quad (1)$$

Here

$$\frac{d}{dt} = \frac{\partial}{\partial t} + \frac{1}{a\sin\theta}\frac{\partial}{\partial\lambda} + \frac{1}{a}\frac{\partial}{\partial\theta} \ ,$$

is the total derivative, u, v are the physical components of the velocity vector, $\Phi = gz$ is the geopotential, z is the height, g is the gravitational acceleration, $f = 2\Omega\cos\theta$ is the Coriolis parameter, Ω is the modulus of angular velocity of Earth's rotation, a is the Earth's radius.

Using Cartesian coordinates of any conformal projection, the equations (1) can be represented as follows (Williamson 1979):

$$\frac{dU}{dt} - \left[f + \left(-V\frac{\partial m}{\partial x} + U\frac{\partial m}{\partial y}\right)\right]V = -m\frac{\partial\Phi}{\partial x} \ ,$$

$$\frac{dV}{dt} + \left[f + \left(-V\frac{\partial m}{\partial x} + U\frac{\partial m}{\partial y}\right)\right]U = -m\frac{\partial\Phi}{\partial y} \ ,$$

$$\frac{d\Phi}{dt} = -\Phi m^2\left[\frac{\partial(U/m)}{\partial x} + \frac{\partial(V/m)}{\partial y}\right] \ . \quad (2)$$

Here the total derivative is defined as

$$\frac{d}{dt} = \frac{\partial}{\partial t} + mU\frac{\partial}{\partial x} + mV\frac{\partial}{\partial y} \ ,$$

where, U and V are the physical components of velocity with respect to axes x and y, and function $m(x, y)$ is the mapping factor (scale function) defined as the ratio between elementary arc lengths along plane curve and respective spherical curve. One can see that the shallow water equations keep a simple form under conformal transformation.

The shallow water equations have the similar form also in rotated spherical coordinates and Cartesian coordinates of arbitrary oblique conformal mapping. Indeed, geometrically the rotated spherical coordinates differ from geographical ones only by choice of the Poles and the first meridian. Algebraic formulas relating these coordinates have the form

$$\begin{cases}\cos\lambda'\sin\theta' = \cos\theta_0\sin\theta\cos(\lambda - \lambda_0) - \sin\theta_0\cos\theta \\ \sin\lambda'\sin\theta' = \sin\theta\sin(\lambda - \lambda_0)\end{cases} \ ,$$

where λ' and θ' are the rotated spherical coordinates, and $P_0 = (\lambda_0, \theta_0)$ is the new "North Pole" in the rotated coordinates. It is simple to show that the equations (1) keep the same form in the rotated coordinates except for definition of the velocity components and the Coriolis parameter (McDonald and Bates 1989). Since oblique conformal mapping is the polar one for the rotated spherical coordinates, the shallow water equations in the Cartesian coordinates of any oblique conformal projection have the form (2) with respective definition of the velocity components and Coriolis parameter.

Let us consider the "ideal" physically uniform grid with mesh size h_0 and another computational grid uniform in Cartesian coordinates (x, y) used for discretization of (2) with mesh size h_1. The real (physical) approximation is the best in the points of computational grid where mapping factor m reaches maximum values m_{max} and it is the worst in the points with minimum values m_{min}. If we assume that the overall accuracy of a numerical scheme is defined by regions with the greatest physical mesh size, then it is necessary to choose computational mesh size $h_1 \approx h_0 \cdot m_{min}$ to guarantee the approximation equivalent to real physical mesh size h_0. Different schemes approximating the system (2) have the maximum allowable time step expressed by formula

$$\tau_{max} \approx \frac{h_1}{m_{max} \cdot s} = \frac{m_{min}}{m_{max}} \cdot \frac{h_0}{s} \ ,$$

where s is the velocity of gravity waves in the case of explicit schemes (for example, leap-frog scheme), or maximum of wind velocity modulus for semi-implicit Eulerian schemes (for example,

Robert's scheme), or maximum variation of wind velocity in the case of semi-implicit semi-Lagrangian schemes (Mesinger and Arakawa 1976, Staniforth and Côté 1991, Durran 1999). Therefore, the number of time steps increases

$$\alpha = \frac{m_{max}}{m_{min}} \qquad (3)$$

times, comparing with the ideal physically homogeneous resolution ($m \equiv 1$) and, consequently, the same scheme on the computationally homogeneous grid takes α times more computations than on the ideal (physically homogeneous) grid where $\alpha = 1$. Two projections are considered equivalent on chosen domain if their variation coefficients are equal. If the form of primitive equations is equivalent in different coordinates, hence, the problem of optimization of the coordinate system consists of finding a projection type with minimum value of variation coefficient α. This is the case of polar and oblique conformal mappings, including the mostly used stereographic, conic and cylindrical projections.

3. SOME THEORETICAL RESULTS ON MINIMIZATION PROBLEM

For subsequent references, let us recall some basic formulas of the specific conformal mappings. The stereographic tangent projection of the sphere of radius a onto a plane with Cartesian coordinates x,y can be written in the form (Williamson 1979, Pearson 1990, Bugayevskiy and Snyder 1995)

$$x = 2a\tan\frac{\theta}{2}\cos\lambda \ , \ y = 2a\tan\frac{\theta}{2}\sin\lambda \ ,$$
$$\lambda \in [0,2\pi), \ \theta \in (0,\pi) \ and \ \theta = 0 \ (or \ \theta = \pi) \ . \ (4)$$

The set of the conic conformal projections tangent to the sphere at the points of colatitude θ_0 (from $(0,\pi/2)$) is defined as follows (Pearson 1990, Bugayevskiy and Snyder 1995)

$$x = a\frac{\sin\theta_0}{n}\left(\tan\frac{\theta}{2}\Big/\tan\frac{\theta_0}{2}\right)^n\cos n\lambda \ ,$$

$$y = a\frac{\sin\theta_0}{n}\left(\tan\frac{\theta}{2}\Big/\tan\frac{\theta_0}{2}\right)^n\sin n\lambda \ ,$$
$$\lambda \in [0,2\pi), \ \theta \in (0,\pi), \qquad (5)$$

where $n = \cos\theta_0 \in (0,1)$ is the parameter specifying the mapping of this set.

The cylindrical conformal mapping tangent to the sphere at the points of the equator has the form (Williamson 1979, Pearson 1990, Bugayevskiy and Snyder 1995)

$$x = a\lambda \ , \ y = a\ln\cot\frac{\theta}{2} \ ,$$
$$\lambda \in [0,2\pi), \quad \theta \in (0,\pi). \qquad (6)$$

The respective mapping factors of the above projections can be expressed as follows (Williamson 1979, Pearson 1990, Bugayevskiy and Snyder 1995):

$$m_{str} = \frac{2}{1+\cos\theta} \ , \qquad (7)$$

$$m_{con} = \frac{\sin\theta_0}{\sin\theta}\left(\tan\frac{\theta}{2}\Big/\tan\frac{\theta_0}{2}\right)^n \ , \qquad (8)$$

and

$$m_{cyl} = \frac{1}{\sin\theta} \ . \qquad (9)$$

In (Bourchtein and Bourchtein 2003) it was proved the principal inequality

$$\alpha_{str} < \alpha_{cyl} < \alpha_{con} \ ,$$

which allows to compare these three groups of mappings and shows that the stereographic mapping tangent to the sphere at the central point of the considered domain Ω is the best choice whatever location and extention of a spherical domain are selected.

Now we can strengthen this result for one special case of the spherical domain. Let us consider the spherical disk Ω_γ of the spherical radius $a\gamma$ ($\gamma \in (0,\pi)$) consisting of all sphere points $P = (a,\lambda,\theta)$ whose spherical (geodesic) distance from the centerpoint $P_0 = (a,\lambda_0,\theta_0)$ is less than $a\gamma$: $d_S(P_0,P) \le a\gamma$. By definition, the distance between sphere points P_0 and P is the length of the shorter great circle arc joining these points.

In what follows we need the following Chebyshev-Milnor theorem (Milnor,1969): if Ω is a simply connected open spherical domain bounded by a twice differentiable curve, then there exists one and, up to a similarity transformation of the plane, only one conformal mapping which minimizes the variation coefficient (3). The "best possible" conformal mapping is characterized by the property that its scale function m is constant along the boundary of Ω.

A direct application of this theorem shows that found in (Bourchtein and Bourchtein 2003) the stereographic projection tangent to the spherical disk Ω_γ at the centerpoint P_0 has the minimum variation coefficient in the entire class of conformal mappings. In fact, since the spherical disk is of required geometry and smoothness, the theorem assures existence of the "best possible" mapping. With no loss of generality we can consider the centerpoint P_0 be the North Pole (otherwise, it is sufficient to apply the theorem in rotated spherical coordinates). Evidently, the above chosen stereographic mapping has the constant value

mapping factor $m = 2/(1 + \cos\gamma)$ on the disk boundary $\partial\Omega_\gamma$. Therefore, this mapping has the minimum variation coefficient α.

Given mapping factor m, the problem of finding the coordinate functions of the "best possible" conformal mapping consists of solution to the following first order non-linear partial differential equations (Bugayevskiy and Snyder 1995):

$$h_\lambda{}^2 + \sin^2\theta \cdot h_\theta{}^2 = a^2 \sin^2\theta \cdot m^2, \quad h = x, y. \quad (10)$$

Except for the above case of the stereographic mapping, we do not know another analytical solution to equation (10) useful for grid generation.

4. APPROXIMATE SOLUTIONS FOR CONFORMAL MAPPINGS

Although the analytical results regarding minimization of variation coefficient are very scarce, some information about mapping properties can be obtained by applying the following results of the Chebyshev-Milnor theory (Milnor, 1969): the mapping factor m associated with a conformal mapping h on a simply connected open spherical domain Ω determines h up to a (orientation preserving or reversing) rigid motion of the plane. A given positive real-valued function m on Ω is the mapping factor associated with some conformal mapping h if, and only if, m is twice differentiable and satisfies the differential equation

$$a^2 \Delta \ln m = 1 \ in \ \Omega,$$

where Δ is the Laplace operator.

Since usually the computational domain is rectangle, it is of practical interest to find out what happens if a spherical domain has rectangular image in the plane. First we find the "best" mapping factor for a spherical domain projected onto square S centered at the origin of planar coordinates and compare the obtained result with that of the "best" stereographic mapping. To this end, according to the Chebyshev-Milnor theory, we should solve the following boundary value problem for the function $g = \ln m$:

$$\Delta g = a^{-2} \ in \ \Omega, \quad g = 0 \ on \ \partial\Omega, \quad (11)$$

where $\partial\Omega$ is the boundary of the domain Ω.
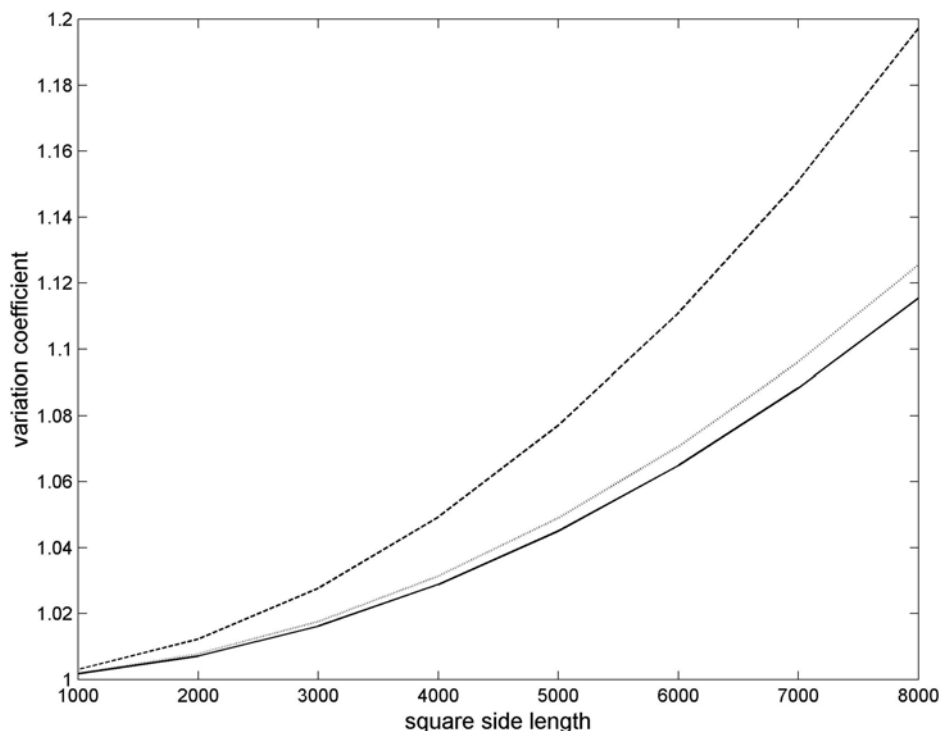
Figure 1. Variation coefficient of the "best possible" and stereographic mappings for the computational square. Each line represents the variation coefficient plotted as a function of the square side length d: solid line is for the "best" conformal mapping, dashed line is for the stereographic mapping and dotted line is for stereographic mapping optimized for the respective disk of the same area.

Since the spherical geometry of the domain Ω, which has the square image S on the plane, is not simple, we transform the problem (11) to the planar one by applying auxiliary stereographic mapping:

$$\Delta g \equiv g_{xx} + g_{yy} = \frac{1}{m_{str}^2 a^2} = \frac{16a^2}{\left(4a^2 + x^2 + y^2\right)^2}$$

$$in\ S\ ,\quad g = 0\ \ on\ \partial S\ . \tag{12}$$

It is well-known that this problem has the unique solution in the class of twice differentiable functions (actually, the solution is analytical function) (e.g., Evans 1998). Though the last problem can be solved analytically in the form of Fourier series, the most simple and accurate way to obtain the solution is the application of standard numerical techniques. For example, a second-order finite-difference approximation followed by the successive overrelaxation method supply a sufficiently accurate solution.

The results of the computation of the variation coefficient for the "best possible" conformal mapping are shown in Fig.1 as a function of the length d of the square side (solid line). It can be compared with the variation coefficient of the stereographic mapping (dashed line). Also the variation coefficient of the stereographic mapping whose image is the planar disk of the radius $d/\sqrt{\pi}$ is plotted (dotted line). This disk has the same area as the respective square. As it was expected, the two lines for the best mappings onto the square and disk domains are sufficiently close. The difference between the best and stereographic mappings for the square domain becomes to be apparent for the square side lengths greater than 6000km.

Similar computations were performed for rectangular domains with the greater/smaller side ratio 3/2 and 2/1. The rectangular computational domains are common in the regional atmospheric modeling based on both finite difference and finite element methods. The obtained results are shown in Figs. 2 and 3. Qualitatively the situation is the same as for the square image, but the differences are greater due to the size of the rectangles.
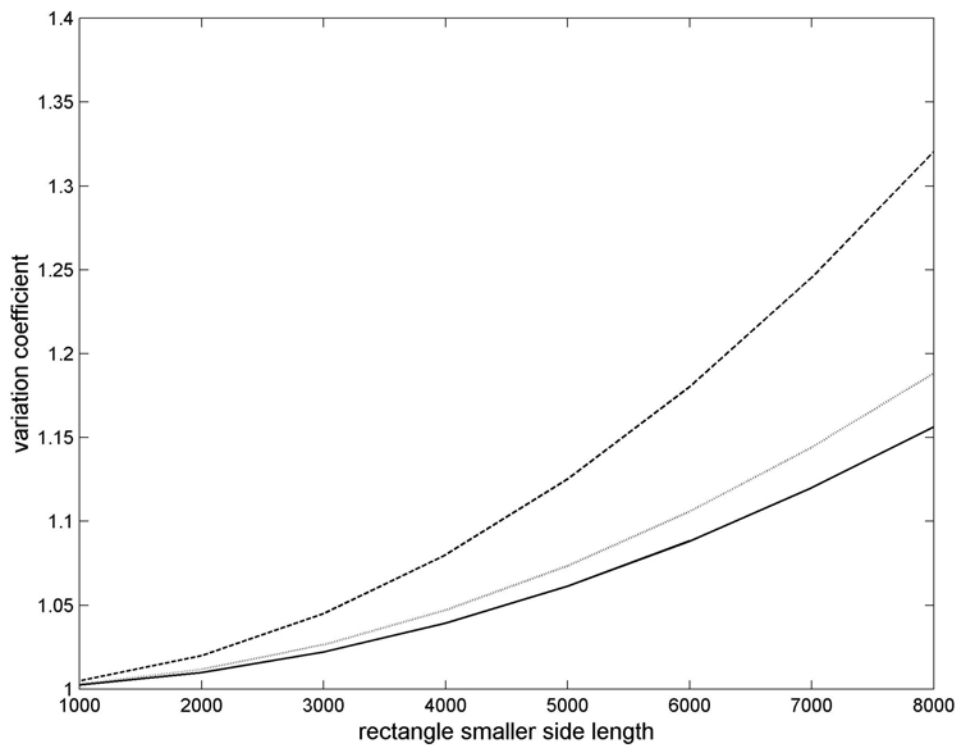
Figure 2. The same as Fig.1, except for computational rectangle with smaller side length d and ratio 3/2 between greater and smaller sides.
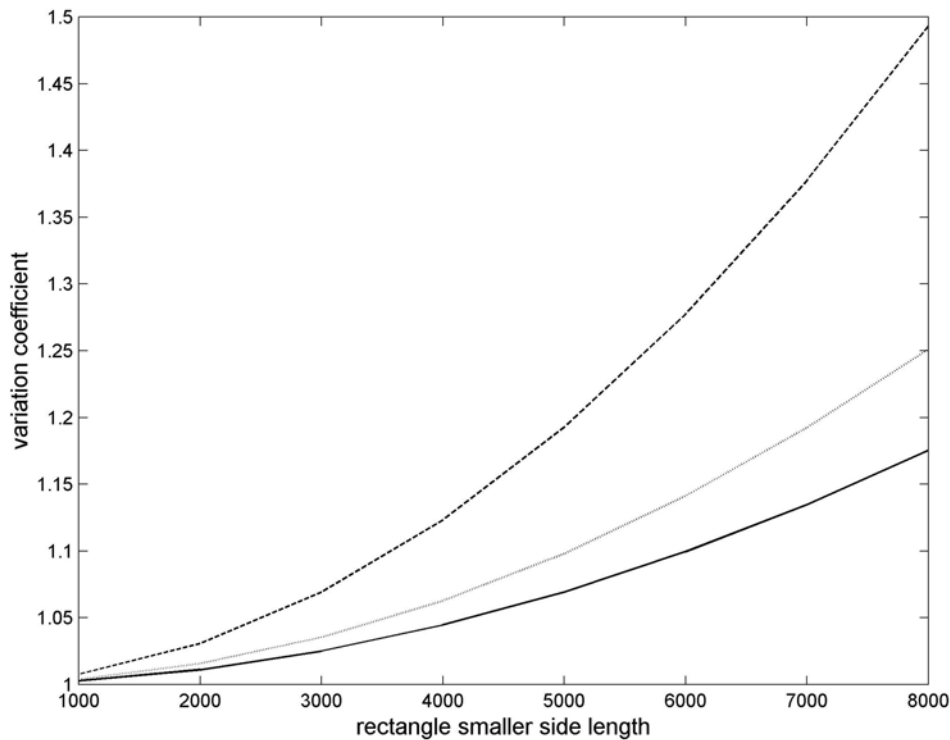
Figure 3. The same as Fig.1, except for computational rectangle with smaller side length *d* and ratio 2/1 between greater and smaller sides.

Finally, we evaluate the mapping characteristics on South America region. Using the rectangular domain on the image plane, which contains the planar image of the South America, we obtain the variation coefficients for different mappings shown in the first line of Table 1. If we restrict the mapping to only South America territory, then the approximate values of α are given in the second line. The third option is related to the case when one is interested in atmospheric modeling over all South America territory. It is well-known that the lateral boundaries of regional models must be removed from the area of interest at least about 1000km for 24-h forecast, because near-boundary regions are strongly affected by boundary conditions supplied by another model (Anthes et al. 1989, Staniforth 1997). In this case it increases significantly the overall extension of the modeling territory, which reflects in a greater variability of variation coefficients. The third line represents the results of this simulation and one can see that the differences among variation coefficients can not be disregarded.

To solve the last two problems we have used the geographical coordinates of the South America contour with the step of 2.5 degrees. These data was projected on planar domain and consecutive points were jointed piecewise linearly forming this way a polygonal domain.

The problem (12) was solved on the polygon using a more complex version of the above mentioned iterative method with the steps of 250km and 500km. The same computations were made with boundary points resolution of 5 degrees. Since the obtained results were quite close we believe the shown values are the good approximations to exact solution of minimization problem.

Table 1. Comparison of the variation coefficients. The columns form the second to fifth contain the results for the best possible, stereographic, cylindrical and conic conformal mappings, respectively; R – rectangular domain, SA – South America, SA+ - South America and adjacent regions.

Domain	best	stereogr	cylindr	conic
R	1.076	1.156	1.221	1.315
SA	1.028	1.138	1.221	1.276
SA+	1.059	1.243	1.397	1.454

Let us note that each time we have used the most optimal variant of the indicated class of mappings. For example, the stereographic mapping means such stereographic projection which assures the minimum variation coefficient among all (polar and oblique, tangent and secant) stereographic mappings. As it was shown in (Bourchtein and Bourchtein 2003) this

1688

is stereographic mapping tangent to sphere at the central point of the chosen domain. If one choose the traditional stereographic mapping perpendicular to the pole axis and secant at the central latitude of the domain, then the results are much worse: for the South America with adjacent areas territory the variation coefficient of such mapping is about 3.0. Similar results can be obtained for non-optimal cylindrical and conic conformal mappings: the traditional cylindrical mapping (tangent or secant) with cylinder axis parallel to polar one gives $\alpha_{cyl} = 2.274$ and standard conic mapping tangent at the central latitude or secant at the middle latitudes of the chosen region gives $\alpha_{cyl} = 1.653$.

5. COMPARISON BETWEEN CONFORMAL AND ORTHOGONAL MAPPINGS

In the last decade, the growing interest in more flexible computational grids gave rise to the application of more general mappings than conformal ones, in particular, to the use of orthogonal mappings, which still maintain a simpler form of the hydrodynamic equations (Rancic et. al. 1996, Murray 1996, Cote 1997, Fox-Rabinovitz et.al. 2000, Kernkamp et.al. 2005). For this reason, it is useful to compare the "best" conformal and orthogonal mappings. To this end, we should to generalize the concepts of the mapping factor and variation coefficient because they are not applied for more general mappings than conformal ones.

Let $d_E(A,B)$ denote the Euclidean distance between the points A and B in the plane. The scale of a mapping h with respect to a pair of distinct points P and Q in the spherical domain Ω is defined to be the ratio

$$\frac{d_E(h(P),h(Q))}{d_S(P,Q)} .$$

The minimum (maximum) scale σ_{min} (σ_{max}) is defined as the infimum (supremum) of the above ratio over all pairs of distinct points in Ω. The next concept is a generalization of the concept of the variation coefficient for non-conformal projections: the distortion δ of the mapping h is the ratio of maximum scale to minimum scale, that is, $\delta = \sigma_{max}/\sigma_{min}$.
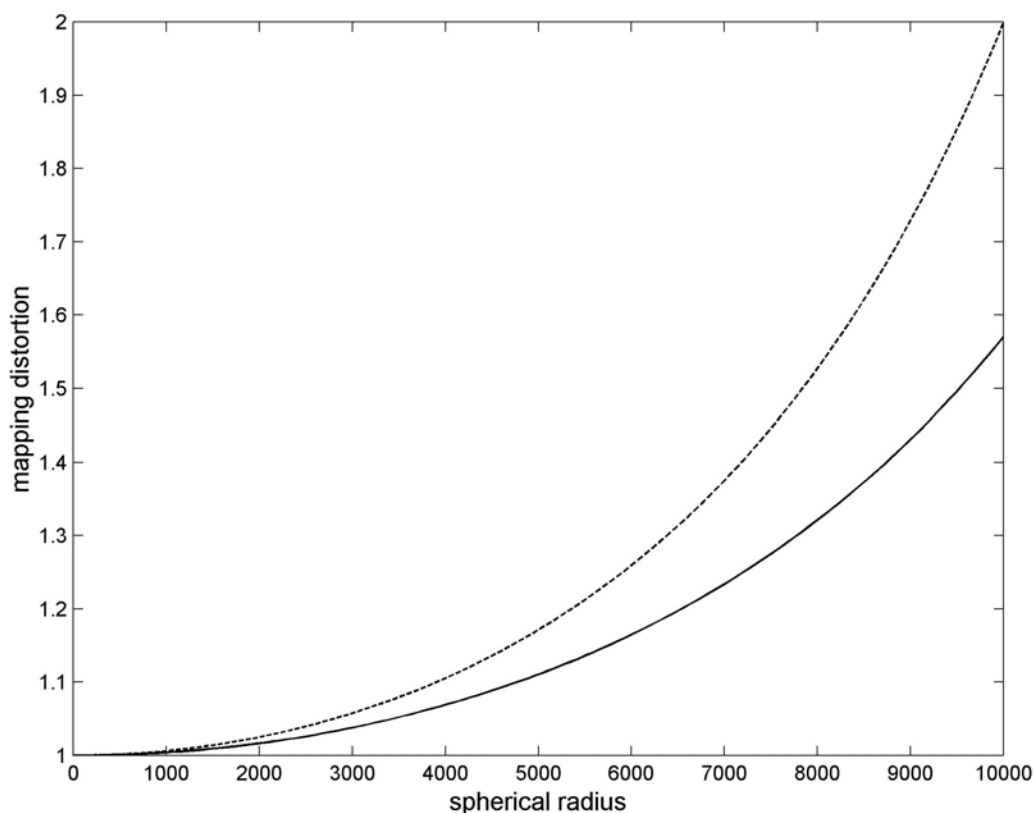
Figure 4. Distortion of the azimuthal equidistant and stereographic mappings for the spherical disk. Each line represents the distortion plotted as a function of the spherical radius: solid line is for the azimuthal equidistant projection and dashed line is for the "best" stereographic mapping.

A minimum distortion mapping h_0 on Ω is a map projection whose distortion δ_0 is less than or equal to the distortion of every other mapping on Ω. Milnor (1969) has proved that the minimum distortion mapping exists in the class of orthogonal mappings and for spherical disk Ω_γ this mapping is azimuthal equidistant projection with distortion

$$\delta_0 = \frac{\gamma}{sin\gamma} \ .$$

Again it is sufficient to consider the spherical disk centered at the North Pole. In this case the azimuthal equidistant mapping is defined by formulas (Pearson 1990, Bugayevskiy and Snyder 1995)

$$\varphi = \lambda \ , \ r = a\theta \ ,$$

and it is orthogonal (but non-conformal) mapping that carries each longitude into a straight line passing through the origin in the plane, and each latitude into a circle centered at the origin.

In Fig.4 we plot the distortion of the azimuthal equidistant and conformal mappings as a function of the spherical radius $a\gamma$. It can be seen that orthogonal mappings assure visibly better uniformity than conformal ones for the spherical radius greater than 5000km. If the spherical radius is smaller than 4000km, then the difference between two projections can be ignored.

To the best of our knowledge, there are no analytical or numerical results about the minimum distortion mappings for other domains. So we have no possibility to compare the best conformal and orthogonal mappings for rectangular domains or for South America region

REFERENCES

Anthes, R.A., Kuo, Y.H., Hsie, E.Y., Low-Nam, S., and Bettge, T.W., 1989: Estimation of skill and uncertainty in regional numerical models. *Q. J. R. Meteorol. Soc.*, **115**, 763-806

Bates, J.R., S. Moorthi, and R.W. Higgins, 1993: A global multilevel atmospheric model using a vector semi-Lagrangian finite-difference scheme. Part I: Adiabatic formulation. *Mon. Wea. Rev.*, **121**, 244-263.

Benoit, R., M. Desgagne, P. Pellerin, S. Pellerin, Y. Chartier, and S. Desjardins, 1997: The Canadian MC2: a semi- Lagrangian, semi-implicit wideband atmospheric model suited for finescale process studies and simulation. *Mon. Wea. Rev.*, **125**, 2382-2415.

Bourchtein, A., 2002: Semi-Lagrangian semi-implicit space splitting regional baroclinic atmospheric model. *Appl. Numer. Math.*, **41**, 307-326.

Bourchtein, A., and L. Bourchtein, 2003: Comparative analysis of conformal mappings used in limited area models of numerical weather prediction. *Mon. Wea. Rev.*, **131**, 1759-1768.

Bugayevskiy, L.M., J.P. Snyder, 1995: *Map projections. A reference manual*. Taylor and Francis, 328pp.

Côté, J., 1997: Variable resolution techniques for weather prediction. *Meteorol. Atmos. Phys.*, **63**, 31-38.

Durran, D.R., 1999: *Numerical methods for wave equations in geophysical fluid dynamics.* Springer-Verlag, 465 pp.

Evans, L.C., 1998: *Partial differential equations.* AMS, 662pp.

Fox-Rabinovitz, M.S., G. L. Stenchikov, M. J. Suarez, L. L. Takacs, and R. C. Govindaraju, 2000: A uniform- and variable-resolution stretched-grid GCM dynamical core with realistic orography. *Mon. Wea. Rev.*, **128**, 1883–1898.

Grell, G.A., J. Dudhia, and D.R. Stauffer, 1994: A description of the fifth generation Penn State/NCAR mesoscale model (MM5). *NCAR Tech. Note NCAR/TN-398+STR*, 138pp.

Kernkamp, H.W.J., H.A.H. Petit, H. Gerritsen, and E.D. Goede, 2005: A unified formulation for the three-dimensional shallow-water equations using orthogonal coordinates: theory and application. *Ocean Dynamics*, **55**, 542-561.

Leslie, L.M., and Purser, R.J., 1991: High-order numerics in an unstaggered three-dimensional time-split semi-Lagrangian forecast model. *Mon. Wea. Rev.* **119**, 1612-1623.

MacDonald, A.E., J.L. Lee, and S. Sun, 2000: QNH: design and test of a quasi-nonhydrostatic model for mesoscale weather prediction. *Mon. Wea. Rev.*, **128**, 1016-1036.

McDonald, A., and J.R. Bates, 1989: Semi-Lagrangian integration of a gridpoint shallow water model on the sphere. *Mon. Wea. Rev.*, **117**, 130-137.

McDonald, A., and J.E. Haugen, 1992: A two time-level, three-dimensional semi-Lagrangian, semi-implicit, limited-area, grid-

point model of the primitive equations. *Mon.Wea. Rev.*, **120**, 2603-2621.

Mesinger, F., and A. Arakawa, 1976: Numerical methods used in atmospheric models. *GARP Publ. Ser.*, No.17, Vol.1, WMO-ICSU, 64 pp.

Mesinger, F., S. Nickovic, D. Gavrilov, and D.G. Deaven, 1988: The step-moutain coordinate: model description and performance for cases of Alpine lee cyclogenesis and for a case of Appalachian redevelopment. *Mon. Wea. Rev.*, **116**, 1493-1507.

Milnor, J., 1969: A problem in cartography. *Amer. Math. Monthly*, **76**, 1101-1112

Murray, R.J., 1996: Explicit generation of orthogonal grids for ocean models. *J. Comp. Phys*., **126**, 251-273.

Pearson, F. II, 1990: *Map projections: theory and applications*. CRC Press, 371 pp.

Rancic, M., Purser J.R., Mesinger F., 1996: A global shallow water model using an expanded spherical cube: Gnomonic versus conformal coordinates. *Q. J. R. Meteor. Soc*., **122**, 959-982.

Robert, A., Yee, T.L., Ritchie, H., 1985: A semi-Lagrangian and semi-implicit numerical integration scheme for multilevel atmospheric models. *Mon. Wea. Rev*. **113**, 388-394.

Staniforth, A., and J. Côté, 1991: Semi-lagrangian integration schemes for atmospheric models - A review. *Mon. Wea. Rev*., **119**, 2206-2223.

Staniforth, A., 1997: Regional modeling: A theoretical discussion. *Meteor. Atmos. Phys.*, **63**, 15-29.

Tanguay, M., Simard, A., and Staniforth, A., 1989: A three-dimensional semi-Lagrangian scheme for the Canadian regional finite-element forecast model. *Mon. Wea. Rev*. **117**, 1861-1871.

Williamson, D.L., 1979: Difference approximations for numerical weather prediction over a sphere. *GARP Publ. Ser.*, No.17, Vol.2, WMO-ICSU, 51-123.